Joint fixity effect on structural design of a box wing aircraft

P. O. Jemitola **J. Fielding** **P. Stocking**
p.o.jemitola@cranfield.ac.uk
Department of Aerospace Engineering
Cranfield University
Cranfield, UK

ABSTRACT

A computational study was performed to compare the stress distributions in finite element torsion box models of a box wing structure that result from employing four different wing/end fin joint fixities. All considered wings were trimmed in pitch. The joint fixities refer to the type of attachment that connects the tip of the fore and aft wings to the end fin. Using loads from a vortex lattice tool, the analysis determined the best wing-joint fixity of a statically loaded idealised box wing configuration by comparing the stress distributions resulting from the different wing joints in addition to other essential aerodynamic requirements. Analysis of the wing joint fixity indicates that the rigid joint is the most suitable.

1.0 INTRODUCTION

This study derives from work on a medium range transport box wing aircraft carried out at Cranfield University. The main attraction of the configuration is the potential reduction in total aircraft drag in still air during cruise; Frediani[1] indicates a reduction of 8 to 13%. Studies by Prandtl[2], Munk[3], Wolkovitch[4] and Nangia and Palmer *et al*[5] also highlight the lower induced drag of box wing aircraft as well as its higher wing stiffness compared to conventional cantilever aircraft. Hajela[6] examined the sensitivity of structural weight to wing sweep and dihedral of a joined wing aircraft. The research carried out by Addoms and Spaid[7] on aerofoil sections emphasise the need to use aerofoils that account for the induced flow curvature for biplane configurations. Bagwill and Selberg[8] showed that fore and aft wing tip overlap in plan view reduces overall aerodynamic efficiency.

Paper No. 3594. Manuscript received 7 June 2010, revised version received 15 February 2011, accepted 3 July 2011.

https://doi.org/10.1017/S0001924000005261 Published online by Cambridge University Press

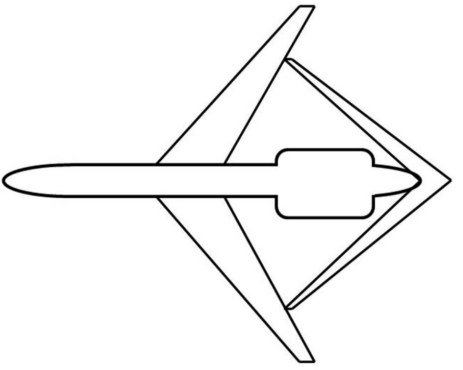


Figure 1. Joined wing configuration.

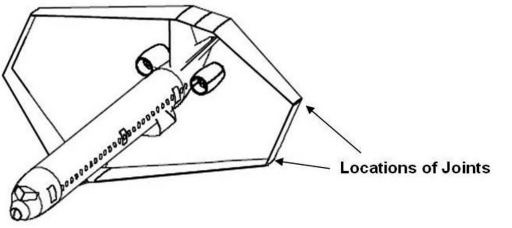


Figure 2. Box wing configuration studied.

In an investigation by Lin *et al*[9] it has been shown that a rigid joint is probably the best in reducing the wing root bending moment and is therefore, the optimum joint fixity for a typical joined wing aircraft configuration as sketched in Fig. 1 (aft wing joined to the fore wing within the semispan). However, they recommend caution when extrapolating their results to other joined-wing configurations. This study draws inspiration from their work and it is instructive to evaluate the type of joint fixity that would be more beneficial for the box wing configuration illustrated in Fig. 2.

Studies were therefore performed to determine the best wing joint fixity of a statically loaded, idealised box wing configuration where both wings produce equal total lift forces. Thus, the internal stress resultants that arise from employing the four joint fixity types shown in Fig. 3 for an assumed flight loading condition were analysed.

2.0 AIRCRAFT DESCRIPTION

The aircraft of study is a 4,000 nautical mile range box wing airliner with a maximum takeoff mass of 127,760kg and wing span of 37·6m. The fore and aft wing gross areas are both 118·32m^2 while the sweep angles are 40º and –25º degrees respectively. Overall fuselage length is 46m and maximum diameter 5·6m. Due to the symmetric nature of the torsion box model, the elastic axis and geometric centres of the wing models coincide and it was along this axis that the loads were applied.

3.0 WING LOADING CONDITIONS

The wing root to wing tip load distributions for the fore and aft wings were obtained from a vortex lattice analysis tool called Athena Vortex Lattice (AVL)[10] and are shown in Fig. 4. AVL is a program that utilises vortex-lattice theory for aerodynamic and dynamic stability analysis of a given aircraft geometry. It uses a vortex lattice model for the lifting surfaces, together with a slender-body model for fuselages and by simulating the flow field, it predicts the pressure distribution around the simulated body. To create a model, AVL requires a text file that defines aircraft geometry. The aircraft is defined as a series of sections running parallel to the chord line. The text file also contains wing and tail surfaces defined in Cartesian co-ordinates.

Sections are needed at root, tip and each end of the wing section or control surface. AVL connects the leading and trailing edges of these sections to create a complete model.

https://doi.org/10.1017/S0001924000005261 Published online by Cambridge University Press

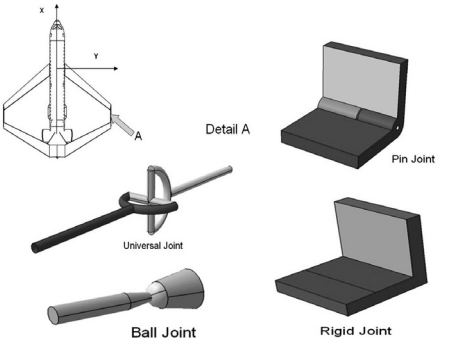


Figure 3. Joint fixity types.

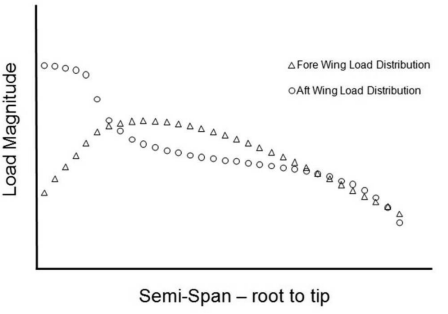


Figure 4. Wing spanwise load distribution.

For the box wing cases, the straight and level 1g condition was imposed before running the AVL simulation. As a consequence, the trim loads were calculated and accounted for by AVL accordingly. In this preliminary analysis, the load distributions by vortex lattice analysis was with equal total lift forces on both wings and the load condition assumed was a 2·5g manoeuvre case limit load at sea level at design diving speed, VD, at maximum take-off weight. In a final design analysis, other loading conditions should also be examined, which include various possible combinations of control deflections and gust loadings.

4.0 FINITE ELEMENT MODEL DESCRIPTION

Due to the simplicity of the torque box and elastic axis beam type models used for the stress/strain analysis, only general stress trends were analysed. These trends were determined as a function of the beam span as opposed to a plane stress or shear flow analysis which would also estimate the stresses around the torque box. Furthermore, as a first approximation only a linear analysis was conducted.

Strand7[(11)] was used for this box wing finite element analysis (FEA). Basically, the Strand7 model consists of any number of structural elements connected by a common control point grid. Several different Strand7 elements could be used to model an aircraft wing. Only beam, plate and brick elements were considered for the box wing finite element model. The beam element was chosen for the box wing model because of the enormous gain in simplicity over a plate or brick model. Beam is a generic name for a group of one-dimensional or line elements.

These elements are all connected between two nodes at their ends and the single dimension is length. Other dimensions can be specified from a range of beam sections available thereby giving three-dimensional properties. In its most general form the beam element can carry axial force, shear force, bending moment and torque. The beam element can also be used to simulate a bar with a non-uniform cross section by interpolating sections. Strand7 has the capability of applying distributed or concentrated loads to a beam element. It also can apply distributed or point torque or moment on beam elements.

Since the box wing configuration analysed in this report is non-uniform (having taper, dihedral and sweep angle), the beam element provides a more practical wing model as opposed to a brick or plate element. Fig. 5 presents a beam version of the box wing model. As the analysis targets conceptualists rather than structural analysts the fuselage is omitted from the idealisation but accounted for by the boundary conditions imposed on the model. Wing inertia relief was

https://doi.org/10.1017/S0001924000005261 Published online by Cambridge University Press

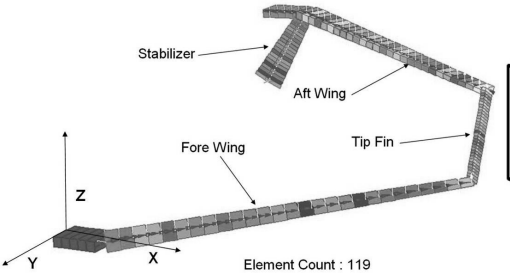


Figure 5. Wing finite element beam model.

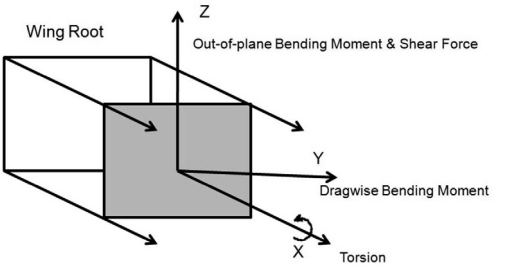


Figure 6. Output parameter definitions.

ignored because its presence or absence was not going to affect the trends observed. In addition, the analysis was conducted with all five cases in iso-inertia conditions (equal to zero). Due to the symmetric nature of the torsion box model, the elastic axis and geometric centres of the wing models coincide and it was along this axis that the loads were applied. For this reason forces and moments are transmitted through the wing tip joints (a single grid point) by equating the respective translations and rotations of the joint receivers at the joint.

The joint fixities were modelled by imposing on the wing tip elements and nodes the translational and rotational freedoms of the joint being modelled. The global coordinate system used for box wing static analysis is defined in Fig. 5. The beam version of the box wing configuration contains 119 elements. Fig. 6 illustrates the output parameter definitions. The out-of-plane bending moment and shear force are in the z-direction while the dragwise bending moment is in the negative y-direction. Torsion is about the x-direction.

5.0 WING CROSS SECTION PROPERTIES

Studies by Wolkovitch[4] indicate that the optimum wing torsion box cross-sectional profile of the box wing configuration is one which accounts for the tilted bending axis of the wings by having the 'bending-resistant material' concentrated near the upper leading edges and lower trailing edges. However, for simplicity, an idealised wing torsion box cross-sectional geometry, illustrated in Fig. 7, was used in this study. Although this is not the optimum torsion box cross section for a box wing, it was assumed to be adequate for the present study. Furthermore, since the wing cross sections are perpendicular to the box wing's elastic axis, the root and tip of the swept wings create modelling problems. However, for slender swept wings and applied loads through the wing elastic axis, an effective wing root and tip may be assumed, simplifying the wing finite element model.

Strand7[11] beam elements require cross sectional properties as program inputs and automatically computes properties such as wing cross sectional area A, the second moments of area Iyy and Izz, and the polar second moment of area, J. Note that for a symmetrical cross section, $Iyz = 0$. The torsion box properties implemented on the model are displayed in Table 1.

The material properties used for all the box wing finite elements are those of Aluminium alloy 2024 – T42 selected from the Strand7 material database; modulus of elasticity, E = 73GPa, modulus of rigidity, G = 27·6GPa, density, ρ = 2,770kg/m^3.

https://doi.org/10.1017/S0001924000005261 Published online by Cambridge University Press

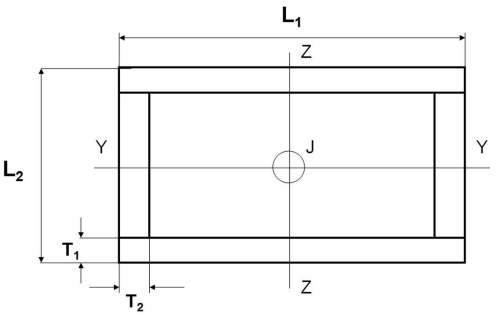


Figure 7. Idealised torsion box cross-section geometry.

Table 1
Torsion box properties

Item	L_2(m)	L_2(m)
Aft Wing Centre	1·84	0·44
Aft Wing Root	1·84	0·44
Tip Fin	0·93	0·22
Fore Wing Root	2·00	0·48
Fore Wing Centre	2·00	0·48
Stabiliser Root	2·06	0·6

6.0 STRUCTURAL SIZING AND FEA PROCEDURE

Sizing was done by implementing the algorithms outlined in Howe[12]. Stiffness criteria that ensure adequate wing aeroelastic performance was accomplished following Howe's approach. The idealised wing structural box model used for the FEA makes the distributed flange construction method ideal for sizing the torsion box skin and web; T_1 and T_2 in Fig. 7.

The structural sizing and FEA procedure for each joint fixity was that a three-dimensional model of the port wing torsion box assembly was built in Strand7[11] with an initial set of values for T_1 and T_2. The loads obtained from AVL[10] were then applied in a distributed manner along the wing's elastic axis and a linear analysis was performed. A second finite element model wing of same joint fixity was then built but with the results of the previous linear analysis implemented in T_1 and T_2. Distributed loads from AVL were then applied and another linear analysis performed with results obtained. These results were then implemented in a third model of the same wing and the procedure repeated until there was less than 1% change in the model's T_1 and T_2 values. This state established the converged solution for that joint fixity wing model. This procedure was performed for all the wing joint fixity models. The shear, torque and bending moments outputs for all the converged solutions of the various joint fixities were obtained and compared.

7.0 RESULTS

The comparative analysis of the moments and forces in the four wing tip joint configurations studied also includes the results of a cantilever wing which was evaluated along with the other joint types. It was basically the fore wing of the box wing configuration with the joint disconnected and provides comparison with the trends of the box wing.

Trim load was estimated and added to the overall mass of the aircraft before running the simulation. AVL 10 was used to shape the lift distribution in order to match the lift and trim together. The parameters evaluated were torque, out-of-plane shear force, out-of-plane bending moment, drag-wise bending moment and wing tip deflection.

Figures 8 and 9 show the torsional load trends in the fore and aft wings for each joint fixity. The applied torsional loads were taken at the elastic axis and moments about the elastic axis of one wing were also caused by the applied loads on the other wing transmitted through the

https://doi.org/10.1017/S0001924000005261 Published online by Cambridge University Press

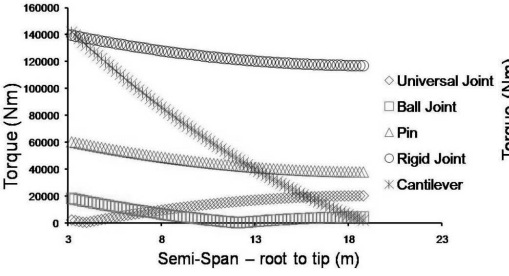


Figure 8. Fore wing torsional force distribution.

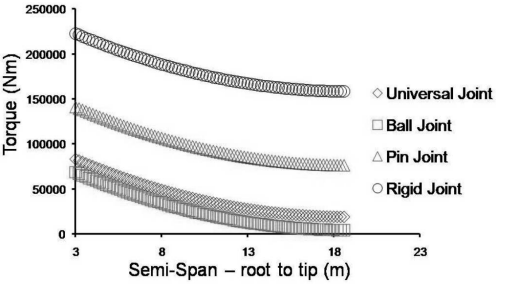


Figure 9. Aft wing torsional force distribution.

wing joint. The exception is the cantilever wing and Fig. 8 shows that the torsional moment falls to zero towards the wing tip in this case. However, of the four joint fixities, the rigid joint produced the largest torsional moment. This is because unlike the universal, pin and ball joints, the rigid joint transmits all moments and forces through the wing joint.

Figures 10 and 11 present the out-of-plane shear force for both fore and aft wings. The trends for all the joints and the cantilever wing are similar. However, for the box wing configuration, the rigid joint produces marginally lower out-of-plane shear stresses than all the other joints on both wings including the cantilever wing.

Figures 12 and 13 represent the out-of-plane bending moment distributions in the fore and aft wings. The trends for the fore and aft wings for all joint types are similar as far as out-of-plane bending moments are concerned. All the joint types show lower wing root bending moment than the cantilever wing. However, the rigid joint shows the greatest reduction of out-of-plane bending moment stresses at the wing root.

Furthermore, the relatively high out-of-plane bending moments produced by the other three joints could make the aft wing susceptible to lateral buckling or divergence and have possibly lower flutter speeds. However, a second non-linear analysis is recommended for future work in identifying post buckling behaviour of the system, as Strand7 is capable of.

The drag-wise bending moment distributions in the fore and aft wings are represented in Figs 14 and 15. It should be noted that the drag-wise bending moment is usually not of significance in a cantilever wing as Fig. 14 highlights. Its prominence in the box wing has to do with the inclined tip fin and sweep of the wings (see Figs 2 and 5).

Under load, the wing tips of the fore and aft wings tend to displace upwards and away from each other. This increases torque moments on the wings as well as generating drag-wise bending moments on both wings. The drag-wise bending moment could therefore be considered in sizing the wing torsion box of box wing aircraft. Furthermore, unlike the three other joints, the rigid joint transmits all the drag-wise bending moment and thus is significantly higher than all the other joint types. Also noteworthy is that in the fore wing

the drag-wise bending moments are significantly higher than at the aft wing and show a steep linear decrease towards the wing tip. At the aft wing the decrease is shallower and this difference could be attributable to the lower sweep angle of the aft wing.

Figures 16 and 17 represent the wing tip deflections for the joint fixities and the cantilever wing. As expected the cantilever wing deflects the most, at almost twice that of the rigid joint. This figure highlights the rigidity of box wing configuration with the rigid joint being the most rigid.

Tables 2 and 3 summarise the results of the relative stress levels for the fore and aft wings.

https://doi.org/10.1017/S0001924000005261 Published online by Cambridge University Press

The wing root values of the joints have been normalised with respect to the respective rigid joint value. For the fore wing all the other joints transmit at least about 26% more out-of-plane bending moment stresses to the wing root than the rigid joint while the cantilever wing transmits 37% more. The ball and universal joints drag-wise bending moments are significantly less than that of the rigid joint at the wing root while the pin joint is about half that of the rigid joint. The trend of the out-of-plane shear force is that all joint types including the cantilever wing are marginally higher than that of the rigid joint. For torsional forces, the rigid joint is similar to the cantilever wing and transmits much higher stresses to the wing root than any of the other joints, with the universal joint transmitting the least amount. As for wing tip deflections, the cantilever wing deflects 81% more than that of the rigid joint box wing configuration. Overall, the universal, ball and pin joints all deflect at least 50% more than the rigid joint.

The aft wing behaves in a similar manner to the fore wing in that all the other joints transmit more than 23% out-of-plane bending moment stresses to the wing root than the rigid joint. Again, the trend for drag-wise bending moment is opposite to the out-of-plane bending moment. The pin and universal joints transmit 7% and 24% less than that of the rigid joint while the universal joint is about 40% the value of the rigid joint. The trends of the out-of-plane shear force show that all the other joints transmit marginally more shear force to the wing root than the rigid joint. All the other joints transmit lower torsional stresses to the wing root than the rigid joint because it transmits all the moments and forces. For the wing tip deflection, the trend is similar to the fore wing with all joints deflecting at least 50% more the rigid joint.

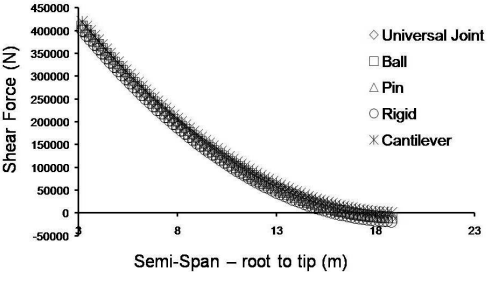


Figure 10. Fore wing out-of-plane shear force distribution.

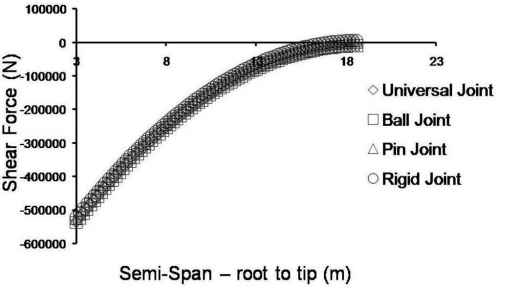


Figure 11. Aft wing out-of-plane shear force distribution.

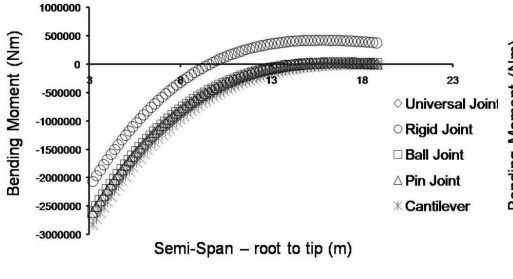


Figure 12. Fore wing out-of-olane bending moment distribution.

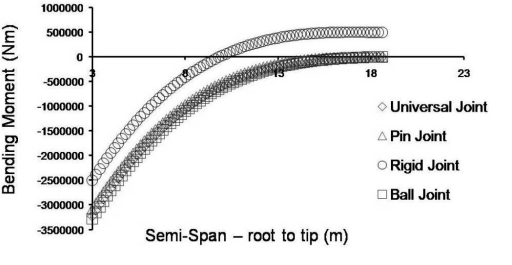


Figure 13. Aft wing out-of-plane bending moment distribution.

https://doi.org/10.1017/S0001924000005261 Published online by Cambridge University Press

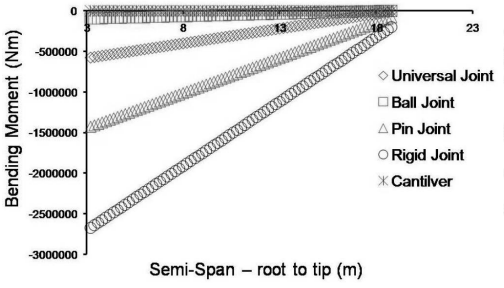


Figure 14. Fore wing drag-wise bending moment distribution.

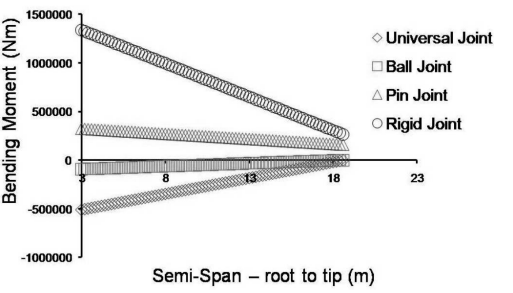


Figure 15. Aft wing drag-wise bending moment distribution.

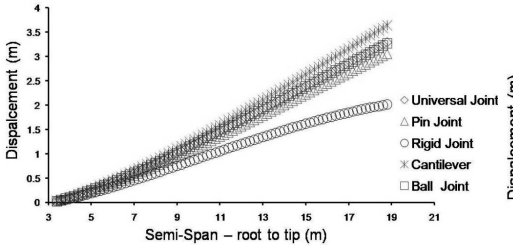


Figure 16. Fore wing deflection.

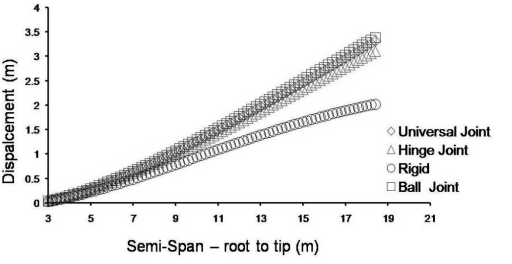


Figure 17. Aft wing deflection.

8.0 THE BEST JOINT FIXITY

In order to determine which joint is best for the box wing configuration it is necessary to outline what criteria the joint should satisfy. It is essential that the joint produces a low overall wing mass; generally lower wing root bending moment suggests lower wing mass. Also, the joint should not in any way accentuate any potential aero elastic problems. It is desirable that the best joint produces greater overall wing stiffness. Since the main merit of this configuration comes from its 'box' nature, it is desirable that the best joint does not allow any structural behaviour that would perturb the aerodynamics of the wing tip/end fin junction, which normally requires special design to maximise the benefits of the configuration. Factors such as flutter and divergence should normally be investigated and compared with strength studies to arrive at the most optimal wing joint fixity for final design considerations, but these are beyond the scope of this work.

It would appear from Tables 2 and 3 that the ball joint would be the best joint for the aircraft. It has the lowest drag-wise bending moment and comparable shear force. It also has a relatively lower torsional force at the wing root which, overall, should make for a light wing. However, the ball joint permits pitching about the flexural axis and about the local stream-wise Y axis at the wing tip. This freedom to pitch as air loads determine is a drawback. Bending and torsion forces contribute to the twist angle of aerofoil sections and are accentuated by aileron deflection. This could lead to decreased aileron effectiveness and even aileron reversal. In addition, the ball joint would interfere in the aerodynamics of the wing tip/end fin junction as it makes for a more flexible wing structure. Hence, the ball joint is unsuitable for the box wing configuration.

https://doi.org/10.1017/S0001924000005261 Published online by Cambridge University Press

Table 2
Normalised wing root parameters – fore wing

Output	Rigid	Universal	Ball	Pin	Cantilever Wing
Out-of-plane BM	1	1·28	1·26	1·26	1·37
Dragwise NBM	1	0·21	0·04	0·53	0·00
Out-of-plane SF	1	1·03	1·02	1.02	1·05
Torsion	1	0·02	0·13	0·43	1·02
Tip Deflection	1	1·64	1·62	1·52	1·81

Table 3
Normalised wing root parameters – aft wing

Output	Rigid	Universal	Ball	Pin
Out-of-plane BM	1	1·29	1·31	1·23
Dragwise NBM	1	0·39	0·07	0·24
Out-of-plane SF	1	1·03	1.03	1.01
Torsion	1	0·37	0·31	0·63
Tip Deflection	1	1·64	1·68	1·54

Even though the universal joint may produce a stiffer wing than the ball joint, it's higher drag-wise bending moment, out-of-plane bending moment and shear force would make for a heavier structure. Furthermore, the universal joint's freedom to pitch about the local stream-wise axis would distort the aerodynamics of the wing tip/end fin junction. The universal joint is therefore unsuitable for the Box wing configuration.

The pin joint's drag-wise bending moment and torsional force, on both wings, are considerably lower than that of the rigid joint wing. However, it's higher wing root bending moment cancels this advantage over the rigid joint. In addition, the joint does not make for the stiffest structure. Furthermore, the movement of the wing tips with respect to the end fin under load would compromise the aerodynamic benefits of the box wing configuration. The pin joint is therefore unsuitable for the box wing configuration.

From the observed trends, the rigid joint should offer a lighter structure than any of the other joints, with its significantly lower wing root out-of-plane bending moment. It is also evident that chord-wise bending moments would be of consideration in sizing the torsion box for wings with this type of joint. However, the joint would not accentuate aero elastic problems and because it transmits all the stresses, it should produce a heavier end fin meaning greater inertia relief. However, this increase in the moment of inertia has a consequence of reduced roll responsiveness; an undesirable development for military aircraft but less critical for civil transports. The rigid joint also produces greater overall wing stiffness which could have ameliorating effects on the reduced roll responsiveness caused by a heavy end fin. Finally, the rigid joint allows for the design of the wing tip/end fin junction to take full advantage of the aerodynamic benefits of the configuration. Consequently, the rigid joint is most suitable for the box wing configuration.

https://doi.org/10.1017/S0001924000005261 Published online by Cambridge University Press

9.0 CONCLUSIONS

The rigid joint was found to be the preferred wing tip/end fin joint type for the box wing configuration. It produced a stiffer, lighter and more aerodynamically advantageous joint. The rigid joint also produces a loading condition on the rear wing which is less likely to promote a stiffness instability in the rear wing. A non-linear analysis is recommended for future work in identifying post buckling behaviour of the system. It is recommended that further studies using wing torsion box cross-sections that account for the tilted bending axis of the wing configuration be investigated. It is also recommended that flutter and divergence analysis of the box wing configuration be performed for a more complete investigation into the effects of the joint fixity.

ACKNOWLEDGMENTS

The author acknowledges the support of the Department of Aerospace Engineering, Cranfield University as well as the technical support of G. Monterzino.

REFERENCES

1. FREDIANI, A. The Prandtlwing, Lecture series on innovative configurations and advanced conceptsfor future civil aircraft ISBN 2-930389-62-1, Von Karman Institute, VKI 2005-06, 2005.
2. PRANDTL, L. Induced drag of multiplanes, *Technische Berichte*, 1924, **III**, (7).
3. MUNK, M. The minimum induced drag of airfoils, Report 121, NACA, March 1923.
4. WOLKOVITCH, J. The joined wing: an overview, *J Aircr*, March 1986, **23**, pp 161-178.
5. NANGIA, R.K., PALMER, M.E. and TILMAN, C.P. Unconventional High Aspect Ratio Joined-Wing Aircraft with Aft and Forward Swept Wing Tips, AIAA-2003-0605, 41st Aerospace Sciences Meeting, Nevada, USA, January 2003.
6. HAJELA, P. Weight Evaluation of the Joined Wing Configuration, CR – 166592, NASA, June 1984.
7. ADDOMS, R.B. and SPAID, F.W. Aerodynamic design of high performance biplane wings, *J Aircr*, August 1975, (12), **8**, pp 629-630.
8. BAGWILL, T. and SELBERG, B. Aerodynamic Investigation of Joined Wing Configurations for Transport Aircraft, AIAA-96/2373, 14th Applied Aerodynamics Conference, Washington DC, USA, June 1996.
9. LIN, H, JHOU, J and STEARMAN R. Influence of Joint Fixity on the Structural Static and Dynamic Response of a Joined-Wing Aircraft, AIAA 90-0980, 31st AIAA/ASME/ASCE/AHS/ASC Structures Structural Dynamics and Materials Conference, Long Beach, California, USA, April 1990.
10. Joined-Wing Aircraft, AIAA 90-0980, 31st AIAA/ASME/ASCE/AHS/ASC Structures Structural Dynamics and Materials Conference, Long Beach, California, USA, April 1990.
11. DRELA, M. and YOUNGREN, H. Athena Vortex Lattice User Manual, Version 3.26, http://web.mit.edu/drela/Public/web/avl/, 2006.
12. Strand7, Release 2.3.8 User's Guide, Strand7 Pty Ltd, 2007.
13. HOWE, D. *Aircraft Loading and Structural Layout*, Professional Engineering Publishing Limited, London, UK, 2004.

https://doi.org/10.1017/S0001924000005261 Published online by Cambridge University Press